An interface crack between two dissimilar functionally graded piezoelectric/piezomagnetic material half infinite planes subjected to the harmonic anti-plane shear stress waves

Zhen-Gong Zhou[a,*] and Biao Wang[b]
[a]*Center for Composite Materials and Structures, Harbin Institute of Technology, P.O. Box 3010, No. 2, Yikuang Street, Harbin, 150001, P.R. China*
[b]*School of Physics and Engineering, Sun Yat-Sen University, Guangzhou 510275, P.R. China*

Abstract. In this paper, the dynamic behavior of an interface crack between two dissimilar functionally graded piezoelectric/piezomagnetic material half infinite planes subjected to the harmonic anti-plane shear stress waves is investigated. To make the analysis tractable, it is assumed that the material properties vary exponentially with coordinate vertical to the crack. By using the Fourier transform technique, the problem can be solved with the help of a pair of dual integral equations in which the unknown variable is the jump of displacements across the crack surfaces. These equations are solved by using the Schmidt method. The relations among the electric filed, the magnetic flux field and the dynamic stress field near the crack tips can be obtained. Numerical examples are provided to show the effect of the functionally graded parameter and the circular frequency of the incident waves upon the stress, the electric displacement and the magnetic flux intensity factors of the crack.

Keywords: Functionally graded piezoelectric/piezomagnetic materials, crack, stress wave

1. Introduction

The magnetoelectric coupling is a new product property of the composites, since it is absent in each constituent. In some cases, the coupling effect of piezoelectric/piezomagnetic composites can be even obtained a hundred times larger than that in single-phase magnetoelectric materials. Consequently, they are extensively used as magnetic field probes, electric packaging, acoustic, hydrophones, medical ultrasonic imaging, sensors, and actuators with the capability of magneto-electro-mechanical energy conversion [1]. The development of piezoelectric/piezomagnetic composites has its roots in the early work of van Suchtelen [2] who proposed that the combination of piezoelectric-piezomagnetic phases may exhibit a new material property – the magnetoelectric coupling effect. Since then, the magnetoelectric coupling effect of $BaTiO_3$-$CoFe_2O_4$ composites has been measured by many researchers. Much of

*Corresponding author. E-mail: zhouzhg@hit.edu.cn.

the theoretical work for the investigation of magnetoelectric coupling effect has only recently been studied [1,3,5–8]. When subjected to mechanical, magnetic and electrical loads in service, these magneto-electro-elastic composites can fail prematurely due to some defects, e.g. cracks, holes, etc. arising during their manufacturing processes. Therefore, it is of great importance to study the magneto-electro-elastic interaction and fracture behaviors of magneto-electro-elastic composites [9–20]. On the other hand, the development of functionally graded materials has demonstrated that they have the potential to reduce the stress concentration and increase of fracture toughness. Consequently, the concept of functionally graded materials can be extended to the piezoelectric/piezomagnetic materials to improve the reliability of piezoelectric/piezomagnetic materials and structures. Some application of functionally graded piezoelectric materials have been made [21,22]. Recently, the fracture problems of functionally graded piezoelectric materials have been considered in [23–28]. Li and Weng [27] first considered the static anti-plane problem of a finite crack in functionally graded piezoelectric material strip. Their results showed that the singular stress and electric displacements in functionally graded piezoelectric materials carry the same forms as those in the homogeneous piezoelectric materials but the magnitudes of the intensity factors depend significantly upon the gradient of the functionally graded piezoelectric materials properties. More recently, Zhou and Wang [29,30] first studied the static ant-plane problems of two parallel cracks and a crack in functionally graded piezoelectric/piezomagnetic materials by using Schmidt method [31]. Their results also showed that the singular stress, the singular electric displacements and the singular magnetic flux in functionally graded piezoelectric/piezomagnetic materials carry the same forms as those in the homogeneous piezoelectric/piezomagnetic materials but the magnitudes of the intensity factors depend significantly upon the gradient of the functionally graded piezoelectric/piezomagnetic materials properties. However, to our knowledge, the dynamic magneto-electro-elastic behavior of functionally graded piezoelectric/piezomagnetic materials with an interface crack subjected to the harmonic anti-plane shear stress waves has not been studied. The present work is an attempt to offer the related information. Here, we give a theoretical solution for this problem.

In this paper, we attempt to extend the concept of functionally graded materials to study the fracture problem of piezoelectric/piezomagnetic materials. The dynamic magneto-electro-elastic behavior of a permeable interface crack between two dissimilar functionally graded piezoelectric/piezomagnetic material half infinite planes subjected to the harmonic anti-plane shear stress waves is investigated using the Schmidt method [31]. To make the analysis tractable, it is assumed that the material properties vary exponentially with coordinate vertical to the crack. Fourier transform technique is applied and a mixed boundary value problem is reduced to a pair of dual integral equations. To solve the dual integral equations, the jump of displacements across the crack surface is expanded in a series of Jacobi polynomials. Numerical solutions are obtained for the dynamic stress, the electric displacement and the magnetic flux intensity factors for permeable crack surface conditions.

2. Formulation of the problem

It is assumed that there is an interface crack of length $2l$ between two dissimilar functionally graded piezoelectric/piezomagnetic material half infinite planes as shown in Fig. 1. It is also assumed that the propagation direction of the harmonic elastic anti-plane shear stress wave is vertical to the crack in functionally graded piezoelectric/piezomagnetic materials. Let ω be the circular frequency of the incident wave. $w_0^{(i)}(x,y,t)$, $\phi_0^{(i)}(x,y,t)$ and $\psi_0^{(i)}(x,y,t)(i=1,2)$ are the mechanical displacement, the electric potential and the magnetic potential, respectively. $\tau_{zk0}^{(i)}(x,y,t)$, $D_{k0}^{(i)}(x,y,t)$ and $B_{k0}^{(i)}(x,y,t)$ $(k =$

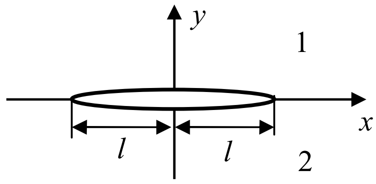

Fig. 1. An interface crack in functionally graded piezoelectric/piezomagnetic materials.

$x, y,\ i = 1, 2)$ are the anti-plane shear stress field, in-plane electric displacement field and in-plane magnetic flux, respectively. Also note that all quantities with superscript $i(i = 1, 2)$ refer to the upper half plane 1 and the lower half plane 2 as shown in Fig. 1, respectively. Because of the incident wave is the harmonic anti-plane shear stress waves, all field quantities of $w_0^{(i)}(x, y, t)$, $\phi_0^{(i)}(x, y, t)$, $\psi_0^{(i)}(x, y, t)$, $\tau_{zk0}^{(i)}(x, y, t)$, $D_{k0}^{(i)}(x, y, t)$ and $B_{k0}^{(i)}(x, y, t)$ can be assumed to be of the forms as follows

$$\begin{aligned}&[w_0^{(i)}(x, y, t), \quad \phi_0^{(i)}(x, y, t), \quad \psi_0^{(i)}(x, y, t), \tau_{zk0}^{(i)}(x, y, t), D_{k0}^{(i)}(x, y, t), B_{k0}^{(i)}(x, y, t)] = \\ &[w^{(i)}(x, y), \quad \phi^{(i)}(x, y), \quad \psi^{(i)}(x, y), \tau_{zk}^{(i)}(x, y), D_k^{(i)}(x, y), B_k^{(i)}(x, y)]e^{-i\omega t}\end{aligned} \tag{1}$$

In what follows, the time dependence of $e^{-i\omega t}$ will be suppressed but understood. The functionally graded piezoelectric/piezomagnetic materials boundary-value problem for the harmonic anti-plane shear waves is considerably simplified if we consider only the out-of-plane displacement, the in-plane electric fields and the in-plane magnetic fields. As discussed in [32,33], since no opening displacement exists for the present anti-plane problem, the crack surfaces can be assumed to be in perfect contact. Accordingly, permeable condition will be enforced in the present study, i.e., the electric potential, the magnetic potential, the normal electric displacement and the magnetic flux are assumed to be continuous across the crack surfaces. Here, the standard superposition technique is used in the present paper. So the boundary conditions of the present problem are (In this paper, we just consider the perturbation field.)

$$\begin{cases}\tau_{yz}^{(1)}(x, 0^+) = \tau_{yz}^{(2)}(x, 0^-) = -\tau_0, |x| \le l \\ \tau_{yz}^{(1)}(x, 0^+) = \tau_{yz}^{(2)}(x, 0^-), w^{(1)}(x, 0^+) = w^{(2)}(x, 0^-), |x| > l\end{cases} \tag{2}$$

$$\begin{cases}\phi^{(1)}(x, 0^+) = \phi^{(2)}(x, 0^-), D_y^{(1)}(x, 0^+) = D_y^{(2)}(x, 0^-) \\ \psi^{(1)}(x, 0^+) = \psi^{(2)}(x, 0^-), B_y^{(1)}(x, 0^+) = B_y^{(2)}(x, 0^-)\end{cases}, \quad |x| \leqslant \infty \tag{3}$$

$$\begin{cases}w^{(1)}(x, y) = w^{(2)}(x, y) = 0 \\ \phi^{(1)}(x, y) = \phi^{(2)}(x, y) = 0 \qquad \text{for} \quad (x^2 + y^2)^{1/2} \to \infty \\ \psi^{(1)}(x, y) = \psi^{(2)}(x, y) = 0\end{cases} \tag{4}$$

where τ_0 is a magnitude of the incident wave.

Crack problems in the non-homogeneous piezoelectric/piezomagnetic materials do not appear to be analytically tractable for arbitrary variations of material properties. Usually, one tries to generate the forms of non- homogeneities for which the problem becomes tractable. Similar to the treatment of the crack problem for isotropic non-homogeneous materials in [21–30,34–36], we assume the material properties are described by:

$$\begin{cases} c_{44}^{(1)} = c_{440}^{(1)} e^{\beta^{(1)} y}, e_{15}^{(1)} = e_{150}^{(1)} e^{\beta^{(1)} y}, \varepsilon_{11}^{(1)} = \varepsilon_{110}^{(1)} e^{\beta^{(1)} y} \\ q_{15}^{(1)} = q_{150}^{(1)} e^{\beta^{(1)} y}, d_{11}^{(1)} = d_{110}^{(1)} e^{\beta^{(1)} y}, \mu_{11}^{(1)} = \mu_{110}^{(1)} e^{\beta^{(1)} y}, \rho^{(1)}(y) = \rho_0^{(1)} e^{\beta^{(1)} y} \\ c_{44}^{(2)} = c_{440}^{(2)} e^{\beta^{(2)} y}, e_{15}^{(2)} = e_{150}^{(2)} e^{\beta^{(2)} y}, \varepsilon_{11}^{(2)} = \varepsilon_{110}^{(2)} e^{\beta^{(2)} y} \\ q_{15}^{(2)} = q_{150}^{(2)} e^{\beta^{(2)} y}, d_{11}^{(2)} = d_{110}^{(2)} e^{\beta^{(2)} y}, \mu_{11}^{(2)} = \mu_{110}^{(2)} e^{\beta^{(2)} y}, \rho^{(2)}(y) = \rho_0^{(2)} e^{\beta^{(2)} y} \end{cases} \tag{5}$$

where $c_{440}^{(i)}$, $e_{150}^{(i)}$, $\varepsilon_{110}^{(i)}$, $q_{150}^{(i)}$, $d_{150}^{(i)}$, $\mu_{110}^{(i)}$, $\rho_0^{(i)}$ and $\beta^{(i)}(i = 1, 2)$ are the shear modulus, the piezoelectric coefficient, the dielectric parameter, the piezomagnetic coefficient, the magnetioelectric coefficient, the magnetic permeability, the mass density and the functionally graded parameter of two dissimilar functionally graded piezoelectric/piezomagnetic material half planes, respectively. Here, the normalized non-homogeneity constants $\beta^{(i)} l(i = 1, 2)$ are varied between -2 and 2, which covers most of the practical cases.

The constitutive equations for the mode III crack can be expressed as follows:

$$\tau_{zk}^{(i)} = c_{44}^{(i)} w_{,k}^{(i)} + e_{15}^{(i)} \phi_{,k}^{(i)} + q_{15}^{(i)} \psi_{,k}^{(i)}, \quad (k = x, y, \quad i = 1, 2) \tag{6}$$

$$D_k^{(i)} = e_{15}^{(i)} w_{,k}^{(i)} - \varepsilon_{11}^{(i)} \phi_{,k}^{(i)} - d_{11}^{(i)} \psi_{,k}^{(i)}, \quad (k = x, y, \quad i = 1, 2) \tag{7}$$

$$B_k^{(i)} = q_{15}^{(i)} w_{,k}^{(i)} - d_{11}^{(i)} \phi_{,k}^{(i)} - \mu_{11}^{(i)} \psi_{,k}^{(i)}, \quad (k = x, y, \quad i = 1, 2) \tag{8}$$

The anti-plane governing equations can be written as follows:

$$\begin{aligned} & c_{440}^{(i)} (\nabla^2 w^{(i)} + \beta^{(i)} \frac{\partial w^{(i)}}{\partial y}) + e_{150}^{(i)} (\nabla^2 \phi^{(i)} + \beta^{(i)} \frac{\partial \phi^{(i)}}{\partial y}) + q_{150}^{(i)} (\nabla^2 \psi^{(i)} + \beta^{(i)} \frac{\partial \psi^{(i)}}{\partial y}) \\ & \quad = -\rho_0^{(i)} \omega^2 w^{(i)} \end{aligned} \tag{9}$$

$$e_{150}^{(i)} (\nabla^2 w^{(i)} + \beta^{(i)} \frac{\partial w^{(i)}}{\partial y}) - \varepsilon_{110}^{(i)} (\nabla^2 \phi^{(i)} + \beta^{(i)} \frac{\partial \phi^{(i)}}{\partial y}) - d_{110}^{(i)} (\nabla^2 \psi^{(i)} + \beta^{(i)} \frac{\partial \psi^{(i)}}{\partial y}) = 0 \tag{10}$$

$$q_{150}^{(i)} (\nabla^2 w^{(i)} + \beta^{(i)} \frac{\partial w^{(i)}}{\partial y}) - d_{110}^{(i)} (\nabla^2 \phi^{(i)} + \beta^{(i)} \frac{\partial \phi^{(i)}}{\partial y}) - \mu_{110}^{(i)} (\nabla^2 \psi^{(i)} + \beta^{(i)} \frac{\partial \psi^{(i)}}{\partial y}) = 0 \tag{11}$$

where $-\rho_0^{(i)} \omega^2 w^{(i)}(x, y) e^{-i\omega t} = \rho_0^{(i)} \frac{\partial^2 w_0^{(i)}(x,y,t)}{\partial t^2} = \rho_0^{(i)} \frac{\partial^2 (w^{(i)}(x,y) e^{-i\omega t})}{\partial t^2}$ and $\nabla^2 = \partial^2/\partial x^2 + \partial^2/\partial y^2$ is the two dimensional Laplace operator.

3. Solutions

Because of the assumed symmetry in geometry and loading, it is sufficient to consider the problem for $0 \leqslant x < \infty$, $-\infty \leqslant y < \infty$ only. The system of above governing Eqs (9)–(11) is solved using the

Fourier integral transform technique to obtain the general expressions for the displacement components, the electric potentials and the magnetic potentials as follows:

$$\begin{cases} w^{(1)}(x,y) = \frac{2}{\pi}\int_0^\infty A_1(s)e^{-\gamma_1^{(1)}y}\cos(sx)ds \\ \phi^{(1)}(x,y) = a_0^{(1)}w^{(1)}(x,y) + \frac{2}{\pi}\int_0^\infty B_1(s)e^{-\gamma_2^{(1)}y}\cos(sx)ds \ , \quad (y \geqslant 0) \\ \psi^{(1)}(x,y) = a_1^{(1)}w^{(1)}(x,y) + \frac{2}{\pi}\int_0^\infty C_1(s)e^{-\gamma_2^{(1)}y}\cos(sx)ds \end{cases} \tag{12}$$

$$\begin{cases} w^{(2)}(x,y) = \frac{2}{\pi}\int_0^\infty A_2(s)e^{\gamma_1^{(2)}y}\cos(sx)ds \\ \phi^{(2)}(x,y) = a_0^{(2)}w^{(2)}(x,y) + \frac{2}{\pi}\int_0^\infty B_2(s)e^{\gamma_2^{(2)}y}\cos(sx)ds \ , \quad (y \leqslant 0) \\ \psi^{(2)}(x,y) = a_1^{(2)}w^{(2)}(x,y) + \frac{2}{\pi}\int_0^\infty C_2(s)e^{\gamma_2^{(2)}y}\cos(sx)ds \end{cases} \tag{13}$$

where $A_1(s)$, $B_1(s)$, $C_1(s)$, $A_2(s)$, $B_2(s)$ and $C_2(s)$ are unknown functions,

$$\gamma_1^{(1)} = \frac{\beta^{(1)} + \sqrt{\beta^{(1)2} + 4[s^2 - \omega^2/c_1^2]}}{2}, \quad \gamma_2^{(1)} = \frac{\beta^{(1)} + \sqrt{\beta^{(1)2} + 4s^2}}{2}, \quad c_1 = \sqrt{\mu_0^{(1)}/\rho_0^{(1)}},$$

$$\mu_0^{(1)} = c_{440}^{(1)} + a_0^{(1)}e_{150}^{(1)} + a_1^{(1)}q_{150}^{(1)}, \quad a_0^{(1)} = \frac{\mu_{110}^{(1)}e_{150}^{(1)} - d_{110}^{(1)}q_{150}^{(1)}}{\varepsilon_{110}^{(1)}\mu_{110}^{(1)} - d_{110}^{(1)2}}, \quad a_1^{(1)} = \frac{q_{150}^{(1)}\varepsilon_{110}^{(1)} - d_{110}^{(1)}e_{150}^{(1)}}{\varepsilon_{110}^{(1)}\mu_{110}^{(1)} - d_{110}^{(1)2}},$$

$$\gamma_1^{(2)} = \frac{\beta^{(2)} + \sqrt{\beta^{(2)2} + 4[s^2 - \omega^2/c_2^2]}}{2}, \quad \gamma_2^{(2)} = \frac{\beta^{(2)} + \sqrt{\beta^{(2)2} + 4s^2}}{2}, \quad c_2 = \sqrt{\mu_0^{(2)}/\rho_0^{(2)}},$$

$$\mu_0^{(2)} = c_{440}^{(2)} + a_0^{(2)}e_{150}^{(2)} + a_1^{(2)}q_{150}^{(2)}, \quad a_0^{(2)} = \frac{\mu_{110}^{(2)}e_{150}^{(2)} - d_{110}^{(2)}q_{150}^{(2)}}{\varepsilon_{110}^{(2)}\mu_{110}^{(2)} - d_{110}^{(2)2}}, \quad a_1^{(2)} = \frac{q_{150}^{(2)}\varepsilon_{110}^{(2)} - d_{110}^{(2)}e_{150}^{(2)}}{\varepsilon_{110}^{(2)}\mu_{110}^{(2)} - d_{110}^{(2)^2}}.$$

So from Eqs (6)–(8), we have

$$\tau_{yz}^{(1)}(x,y) = -\frac{2e^{\beta^{(1)}y}}{\pi}\int_0^\infty \{\mu_0^{(1)}\gamma_1^{(1)}A_1(s)e^{-\gamma_1^{(1)}y} + \gamma_2^{(1)}[e_{150}^{(1)}B_1(s) + q_{150}^{(1)}C_1(s)]e^{-\gamma_2^{(1)}y}\}\cos(sx)ds \tag{14}$$

$$D_y^{(1)}(x,y) = \frac{2e^{\beta^{(1)}y}}{\pi}\int_0^\infty \gamma_2^{(1)}[\varepsilon_{110}^{(1)}B_1(s) + d_{110}^{(1)}C_1(s)]e^{-\gamma_2^{(1)}y}\cos(sx)ds \tag{15}$$

$$B_y^{(1)}(x,y) = \frac{2e^{\beta^{(1)}y}}{\pi}\int_0^\infty \gamma_2^{(1)}[d_{110}^{(1)}B_1(s) + \mu_{110}^{(1)}C_1(s)]e^{\gamma_2^{(1)}y}\cos(sx)ds \tag{16}$$

$$\tau_{yz}^{(2)}(x,y) = \frac{2e^{\beta^{(2)}y}}{\pi}\int_0^\infty \{\mu_0^{(2)}\gamma_1^{(2)}A_2(s)e^{\gamma_1^{(2)}y} + \gamma_2^{(2)}[e_{150}^{(2)}B_2(s) + q_{150}^{(2)}C_2(s)]e^{\gamma_2^{(2)}y}\}\cos(sx)ds \tag{17}$$

$$D_y^{(2)}(x,y) = -\frac{2e^{\beta^{(2)}y}}{\pi}\int_0^\infty \gamma_2^{(2)}[\varepsilon_{110}^{(2)}B_2(s) + d_{110}^{(2)}C_2(s)]e^{\gamma_2^{(2)}y}\cos(sx)ds \tag{18}$$

$$B_y^{(2)}(x,y) = -\frac{2e^{\beta^{(2)}y}}{\pi}\int_0^\infty \gamma_2^{(2)}[d_{110}^{(2)}B_2(s) + \mu_{110}^{(2)}C_2(s)]e^{\gamma_2^{(2)}y}\cos(sx)ds \tag{19}$$

To solve the problem, the jump of displacements across the crack surfaces is defined as follows:

$$f(x) = w^{(1)}(x,0^+) - w^{(2)}(x,0^-) \tag{20}$$

Substituting Eqs (12)–(13) into Eq. (20), and applying the Fourier transform and the boundary conditions (3), it can be obtained

$$\bar{f}(s) = A_1(s) - A_2(s) \tag{21}$$

$$a_0^{(1)}A_1(s) - a_0^{(2)}A_2(s) + B_1(s) - B_2(s) = 0 \tag{22}$$

$$a_1^{(1)}A_1(s) - a_1^{(2)}A_2(s) + C_1(s) - C_2(s) = 0 \tag{23}$$

A superposed bar indicates the Fourier transform throughout the paper. Substituting Eqs (14)–(19) into the boundary conditions (2)–(4), we have

$$\begin{aligned}&\mu_0^{(1)}\gamma_1^{(1)}A_1(s) + \gamma_2^{(1)}[e_{150}^{(1)}B_1(s) + q_{150}^{(1)}C_1(s)] + \mu_0^{(2)}\gamma_1^{(2)}A_2(s)\\&\quad+\gamma_2^{(2)}[e_{150}^{(2)}B_2(s) + q_{150}^{(2)}C_2(s)] = 0\end{aligned} \tag{24}$$

$$\gamma_2^{(1)}[\varepsilon_{110}^{(1)}B_1(s) + d_{110}^{(1)}C_1(s)] + \gamma_2^{(2)}[\varepsilon_{110}^{(2)}B_2(s) + d_{110}^{(2)}C_2(s)] = 0 \tag{25}$$

$$\gamma_2^{(1)}[d_{110}^{(1)}B_1(s) + \mu_{110}^{(1)}C_1(s)] + \gamma_2^{(2)}[d_{110}^{(2)}B_2(s) + \mu_{110}^{(2)}C_2(s)] = 0 \tag{26}$$

By solving six Eqs (21)–(26) with six unknown functions and substituting the solutions into Eqs (14)–(16) and applying the boundary conditions (2)–(3), it can be given:

$$\frac{2}{\pi}\int_0^\infty \bar{f}(s)\cos(sx)ds = 0, \quad x > l \tag{27}$$

$$\frac{2}{\pi}\int_0^\infty g_1(s)\bar{f}(s)\cos(sx)ds = -\tau_0, \quad 0 \leqslant x \leqslant l \tag{28}$$

where $g_1(s)$ is a known function (see Appendix). $\lim\limits_{s\to\infty} g_1(s)/s = \beta_1$. β_1 is a constant which depends on the properties of the materials (see Appendix). However, β_1 is independent of the functionally graded parameters $\beta^{(1)}$ and $\beta^{(2)}$. When the properties of the upper and the lower half planes are continuous along the crack line, $\beta_1 = -c_{440}^{(1)}/2$. The above a pair of dual integral Eqs (27)–(28) must be solved to determine the unknown function $\bar{f}(s)$.

4. Solution of the dual integral equations

The Schmidt method [31] is used to solve the dual integral equations. The jump of displacements across the crack surfaces is represented by the following series:

$$f(x) = \sum_{n=1}^{\infty} b_n P_{2n-2}^{(\frac{1}{2},\frac{1}{2})}(\frac{x}{l})(1-\frac{x^2}{l^2})^{\frac{1}{2}}, \quad \text{for}]0 \leqslant x \leqslant l \tag{29}$$

$$f(x) = w^{(1)}(x,0) - w^{(2)}(x,0) = 0, \text{ for } x > l \tag{30}$$

where b_n are unknown coefficients to be determined and $P_n^{(\frac{1}{2},\frac{1}{2})}(x)$ is a Jacobi polynomial [37]. The Fourier transforms of Eqs (29)–(30) are [38]

$$\bar{f}(s) = \sum_{n=1}^{\infty} b_n G_n \frac{1}{s} J_{2n-1}(sl), \quad G_n = 2\sqrt{\pi}(-1)^{n-1}\frac{\Gamma(2n-\frac{1}{2})}{(2n-2)!} \tag{31}$$

where $\Gamma(x)$ and $J_n(x)$ are the Gamma and Bessel functions, respectively.

Substituting Eq. (31) into Eqs (27)–(28), Eq. (27) has been automatically satisfied. After integration with respect to x in $[0,x]$, Eq. (28) reduces to

$$\frac{2}{\pi}\sum_{n=1}^{\infty} b_n G_n \int_0^{\infty} \frac{1}{s^2} g_1(s) J_{2n-1}(sl)\sin(sx)ds = -\tau_0 x, \quad 0 \leqslant x \leqslant l \tag{32}$$

From the following relationship [37]

$$\int_0^{\infty} \frac{1}{s} J_n(sa)\sin(bs)ds = \begin{cases} \frac{\sin[n\sin^{-1}(b/a)]}{n}, a > b \\ \frac{a^n \sin(n\pi/2)}{n[b+\sqrt{b^2-a^2}]^n}, b > a \end{cases} \tag{33}$$

the semi-infinite integral in Eq. (32) can be modified as:

$$\int_0^{\infty} \frac{1}{s}\left[\beta_1 + (\frac{g_1(s)}{s} - \beta_1)\right] J_{2n-1}(sl)\sin(sx)ds = \frac{\beta_1}{2n-1}\sin\left[(2n-1)\sin^{-1}(\frac{x}{l})\right] + \int_0^{\infty} \frac{1}{s}\frac{g_1(s)-\beta_1 s}{s} J_{2n-1}(sl)\sin(sx)ds \tag{34}$$

It can be seen that the integrands of the semi-infinite integrals in the right end of Eq. (34) tend rapidly to zero. Thus the semi-infinite integral in Eq. (34) can be numerical evaluated easily. Equation (32) can now be solved for the coefficients b_n by the Schmidt method [31]. For brevity, Eq. (32) can be rewritten as follows:

$$\sum_{n=1}^{\infty} b_n E_n(x) = U(x), 0 \leqslant x \leqslant l \tag{35}$$

where $E_n(x)$ and $U(x)$ are known functions and the coefficients b_n are to be determined. A set of functions $P_n(x)$ which satisfy the orthogonality condition

$$\int_0^{l} P_m(x)P_n(x)dx = N_n\delta_{mn}, \quad N_n = \int_0^{l} P_n^2(x)dx \tag{36}$$

can be constructed from the function $E_n(x)$, such that

$$P_n(x) = \sum_{i=1}^{n} \frac{M_{in}}{M_{nn}} E_i(x) \tag{37}$$

where M_{ij} is the cofactor of the element d_{ij} of D_n, which is defined as

$$D_n = \begin{bmatrix} d_{11}, d_{12}, d_{13}, \ldots, d_{1n} \\ d_{21}, d_{22}, d_{23}, \ldots, d_{2n} \\ d_{31}, d_{32}, d_{33}, \ldots, d_{3n} \\ \ldots \\ \ldots \\ \ldots \\ d_{n1}, d_{n2}, d_{n3}, \ldots, d_{nn} \end{bmatrix}, \quad d_{ij} = \int_0^l E_i(x) E_j(x) dx \tag{38}$$

Using Eqs (35)–(38), we obtain

$$b_n = \sum_{j=n}^{\infty} q_j \frac{M_{nj}}{M_{jj}} \quad \text{with} \quad q_j = \frac{1}{N_j} \int_0^l U(x) P_j(x) dx \tag{39}$$

5. Intensity factors

The coefficients b_n are known, so that the entire perturbation stress field, the perturbation electric displacement field and the magnetic flux can be obtained. However, in fracture mechanics, it is of importance to determine the perturbation stress $\tau_{yz}^{(1)}$, the perturbation electric displacement $D_y^{(1)}$ and the magnetic flux $B_y^{(1)}$ in the vicinity of the crack tips. In the case of the present study, $\tau_{yz}^{(1)}$, $D_y^{(1)}$ and $B_y^{(1)}$ along the crack line can be expressed respectively as

$$\begin{aligned} \tau_{yz}^{(1)}(x,0) &= \frac{2}{\pi} \sum_{n=1}^{\infty} b_n G_n \int_0^{\infty} \frac{1}{s} g_1(s) J_{2n-1}(sl) \cos(xs) ds \\ &= \frac{2\beta_1}{\pi} \sum_{n=1}^{\infty} b_n G_n \int_0^{\infty} J_{2n-1}(sl) \cos(xs) ds \\ &\quad + \frac{2}{\pi} \sum_{n=1}^{\infty} b_n G_n \int_0^{\infty} \left[\frac{1}{s} g_1(s) - \beta_1 \right] J_{2n-1}(sl) \cos(xs) ds \end{aligned} \tag{40}$$

$$\begin{aligned} D_y^{(1)}(x,0) &= \frac{2}{\pi} \sum_{n=1}^{\infty} b_n G_n \int_0^{\infty} \frac{g_2(s)}{s} J_{2n-1}(sl) \cos(xs) ds \\ &= \frac{2\beta_2}{\pi} \sum_{n=1}^{\infty} b_n G_n \int_0^{\infty} J_{2n-1}(sl) \cos(xs) ds \\ &\quad + \frac{2}{\pi} \sum_{n=1}^{\infty} b_n G_n \int_0^{\infty} \left[\frac{1}{s} g_2(s) - \beta_2 \right] J_{2n-1}(sl) \cos(xs) ds \end{aligned} \tag{41}$$

$$
\begin{aligned}
B_y^{(1)}(x,0) &= \frac{2}{\pi}\sum_{n=1}^{\infty} b_n G_n \int_0^{\infty} \frac{g_3(s)}{s} J_{2n-1}(sl)\cos(xs)ds \\
&= \frac{2\beta_3}{\pi}\sum_{n=1}^{\infty} b_n G_n \int_0^{\infty} J_{2n-1}(sl)\cos(xs)ds \\
&\quad + \frac{2}{\pi}\sum_{n=1}^{\infty} b_n G_n \int_0^{\infty} \left[\frac{1}{s}g_3(s) - \beta_3\right] J_{2n-1}(sl)\cos(xs)ds
\end{aligned} \tag{42}
$$

where $g_2(s)$ and $g_3(s)$ are known functions (see Appendix). $\lim_{s\to\infty} g_2(s)/s = \beta_2$. $\lim_{s\to\infty} g_3(s)/s = \beta_3$. Where β_2 and β_3 are two constants which depend on the properties of the materials (see Appendix). When the properties of the upper and the lower half planes are continuous along the crack line, $\beta_2 = -e_{150}^{(1)}/2$ and $\beta_3 = -q_{150}^{(1)}/2$.

From the following relationship [37]

$$
\int_0^{\infty} J_n(sa)\cos(bs)ds = \begin{cases} \frac{\cos[n\sin^{-1}(b/a)]}{\sqrt{a^2-b^2}}, a > b \\ -\frac{a^n \sin(n\pi/2)}{\sqrt{b^2-a^2}[b+\sqrt{b^2-a^2}]^n}, b > a \end{cases} \tag{43}
$$

the singular parts of the stress field, the electric displacement and the magnetic flux near the crack tips in Eqs (40)–(42) can be expressed, respectively, as follows ($x > l$):

$$
\tau = -\frac{2\beta_1}{\pi}\sum_{n=1}^{\infty} b_n G_n H_n(x) \tag{44}
$$

$$
D = -\frac{2\beta_2}{\pi}\sum_{n=1}^{\infty} b_n G_n H_n(x) \tag{45}
$$

$$
B = -\frac{2\beta_3}{\pi}\sum_{n=1}^{\infty} b_n G_n H_n(x) \tag{46}
$$

where $H_n(x) = \frac{(-1)^{n-1} l^{2n-1}}{\sqrt{x^2-l^2}[x+\sqrt{x^2-l^2}]^{2n-1}}$.

The stress intensity factor K, the electric displacement intensity factor K^D and the magnetic flux intensity factor K^B can be expressed, respectively, as follows:

$$
K = \lim_{x\to l^+} \sqrt{2(x-l)}\cdot\tau = -\frac{4\beta_1}{\sqrt{\pi l}}\sum_{n=1}^{\infty} b_n \frac{\Gamma(2n-\frac{1}{2})}{(2n-2)!} \tag{47}
$$

$$
K^D = \lim_{x\to l^+} \sqrt{2(x-l)}\cdot D = -\frac{4\beta_2}{\sqrt{\pi l}}\sum_{n=1}^{\infty} b_n \frac{\Gamma(2n-\frac{1}{2})}{(2n-2)!} = \frac{\beta_2}{\beta_1}K \tag{48}
$$

$$
K^B = \lim_{x\to l^+} \sqrt{2(x-l)}\cdot B = -\frac{4\beta_3}{\sqrt{\pi l}}\sum_{n=1}^{\infty} b_n \frac{\Gamma(2n-\frac{1}{2})}{(2n-2)!} = \frac{\beta_3}{\beta_1}K \tag{49}
$$

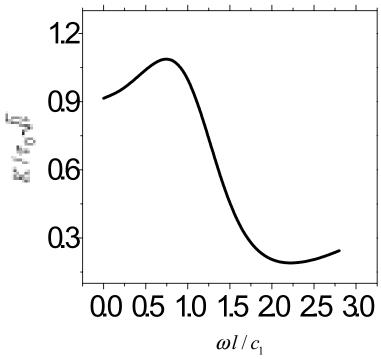

Fig. 2. The stress intensity factor versus $\omega l/c_1$ for $l = 1.0$, $\beta^{(1)}l = 0.2$ and $\beta^{(2)}l = 0.3$ (Material-I/Material-II).

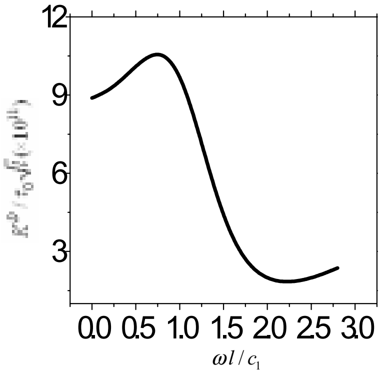

Fig. 3. The electric displacement intensity factor versus $\omega l/c_1$ for $l = 1.0$, $\beta^{(1)}l = 0.2$ and $\beta^{(2)}l = 0.3$ (Material-I/Material-II).

6. Numerical calculations and discussion

From works [29–31], it can be seen that the Schmidt method performs satisfy if the first ten terms of the infinite series Eq. (35) are retained. At $-l \leqslant x \leqslant l$, $y = 0$, it can be obtained that $\tau_{yz}^{(1)}/\tau_0$ is very close to negative unity. Hence, the solution of present paper can also be proved to satisfy the boundary conditions (1). In all computations, according to [9,10,17], the constants of materials-I are assumed to be that $c_{440}^{(1)} = 44.0$ (GPa), $e_{150}^{(1)} = 5.8$ (C/m^2), $\varepsilon_{110}^{(1)} = 5.64 \times 10^{-9}$ (C^2/Nm^2), $q_{150}^{(1)} = 275.0$ (N/Am), $d_{110}^{(1)} = 0.005 \times 10^{-9}$ (Ns/VC), $\mu_{110}^{(1)} = -297.0 \times 10^{-6}$ (Ns^2/C^2), $\rho_0^{(1)} = 1500$ kg/m^3 and the constants of materials-II are assumed to be that $c_{440}^{(2)} = 34.0$ (GPa), $e_{150}^{(2)} = 4.8$ (C/m^2), $\varepsilon_{110}^{(2)} = 4.64 \times 10^{-9}$ (C^2/Nm^2), $q_{150}^{(2)} = 195.0$ (N/Am), $d_{110}^{(2)} = 0.004 \times 10^{-9}$ (Ns/VC), $\mu_{110}^{(2)} = -201.0 \times 10^{-6}$ (Ns^2/C^2), $\rho_0^{(2)} = 1000$ kg/m^3. The results of the present paper are shown in Figs 2–12. From the results, the following observations are very significant:

(i) From the results, it can be shown that the singular stress, electric displacements and the magnetic flux in functionally graded piezoelectric/piezomagnetic materials carry the same forms as those in the homogeneous piezoelectric/piezomagnetic materials or in the homogeneous piezoelectric materials but the magnitudes of the intensity factors depend significantly upon the gradient of the functionally graded piezoelectric/piezomagnetic materials properties as discussed in [27–30].

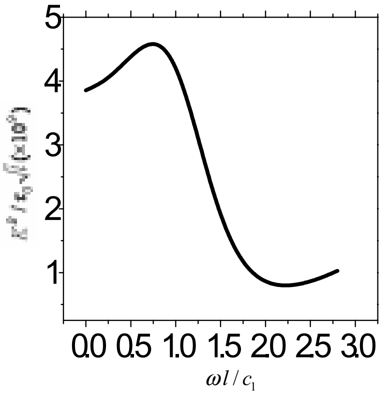

Fig. 4. The magnetic flux intensity factor versus $\omega l/c_1$ for $l = 1.0$, $\beta^{(1)}l = 0.2$ and $\beta^{(2)}l = 0.3$ (Material-I/Material-II).

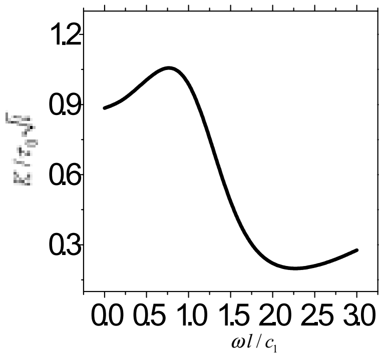

Fig. 5. The stress intensity factor versus $\omega l/c_1$ for $l = 1.0$, $\beta^{(1)}l = 0.4$ and $\beta^{(2)}l = 0.3$ (Material-I/Material-I).

(ii) The electro-magneto-elastic coupling effects can be obtained as shown in Eqs (47)–(49). For the electric displacement and the magnetic flux intensity factors, they have the same changing tendency as the stress intensity factor as shown in Figs 2–4. This might be due to the linearity of the fracture problem. However, the amplitude values of the electric displacement filed, the magnetic flux field and the stress field are different. The amplitude values of the electric displacement and the magnetic flux fields are very small as shown in Figs 3 and 4. The results of the electric displacement and the magnetic flux intensity factors can be directly obtained form the results of the stress intensity factors through Eqs (47)–(49). This means that an applied mechanical load alone can produce the electric displacement and magnetic flux singularities. The results of the electric displacement and the magnetic flux intensity factors of the other cases have been omitted in the present paper.

(iii) The stress, the electric displacement and the magnetic flux intensity factors of crack in the functionally graded materials increase with the increase of the incident wave frequency until reaching a peak and then to decrease in magnitude as shown in Figs 2–6. When the material properties of the upper half plane and the lower half plane alone the crack line are continuous, it can be got the same conclusion as shown in Figs 5–6. In this case, the results are very close to one another showing a weak dependency on the value of $\beta^{(2)}l$. It can be also obtained that this conclusion is the same as the dynamic anti-plane shear fracture problem in the isotropic

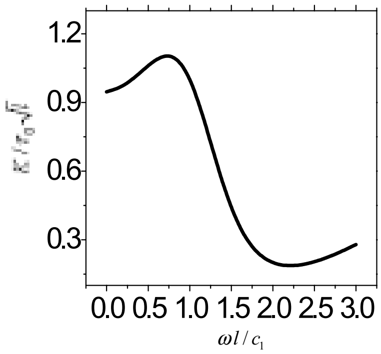

Fig. 6. The stress intensity factor versus $\omega l/c_1$ for $l = 1.0$, $\beta^{(1)}l = 0.4$ and $\beta^{(2)}l = 0.0$ (Material-I/Material-I).

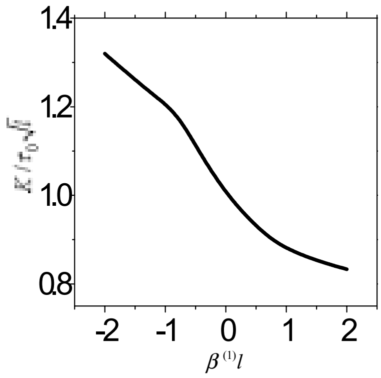

Fig. 7. The stress intensity factor versus $\beta^{(1)}l$ for $l = 1.0$, $\omega l/c_1 = 0.3$ and $\beta^{(2)}l = 0.3$ (Material-I/Material-II).

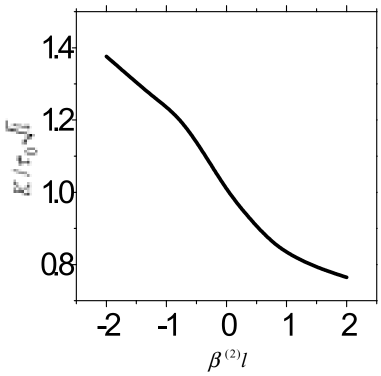

Fig. 8. The stress intensity factor versus $\beta^{(2)}l$ for $l = 1.0$, $\omega l/c_1 = 0.3$ and $\beta^{(1)}l = 0.4$ (Material-I/Material-II).

homogeneous materials as shown in Figs 5–6. From the results, it can be concluded that the stress, the electric displacement and the magnetic fields near the crack tips can be deduced by adjusting the frequency of incident waves in engineering practices.

(iv) The stress intensity factors decrease with the increase in the functionally graded parameters $\beta^{(i)}l$ $(i = 1, 2)$ as shown in Figs 7–12. Form the results as shown in Figs 7–12, it can be obtained that

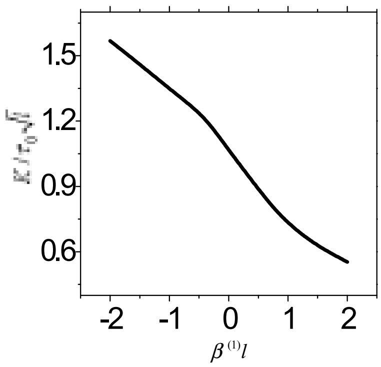

Fig. 9. The stress intensity factor versus $\beta^{(1)}l$ for $l = 1.0$, $\omega l/c_1 = 0.3$ and $\beta^{(2)}l = \beta^{(1)}l$ (Material-I/Material-II).

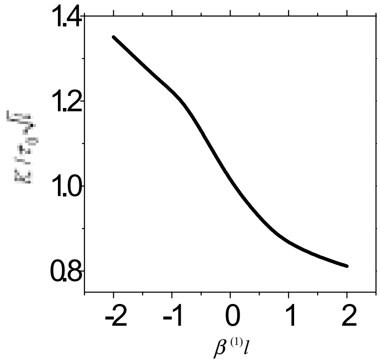

Fig. 10. The stress intensity factor versus $\beta^{(1)}l$ for $l = 1.0$, $\omega l/c_1 = 0.3$ and $\beta^{(2)}l = 0.3$ (Material-I/Material-I).

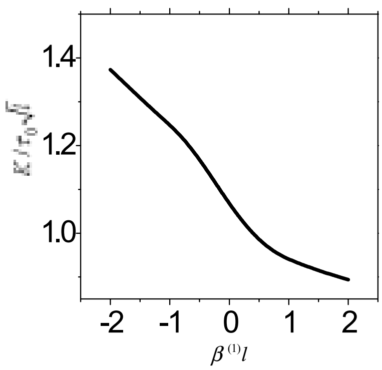

Fig. 11. The stress intensity factor versus $\beta^{(1)}l$ for $l = 1.0$, $\omega l/c_1 = 0.3$ and $\beta^{(2)}l = 0.0$ (Material-I/Material-I).

the stress intensity factors have a similar changing tendency with the variation of $\beta^{(1)}l$ or $\beta^{(2)}l$. When the material properties of the upper half plane and the lower half plane alone the crack line are continuous, it can be got the same conclusion as shown in Figs 10–12. This means that, by adjusting the functionally graded parameters, the dynamic stress fields near the crack tips can be reduced.

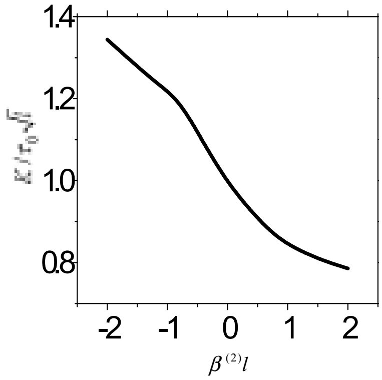

Fig. 12. The stress intensity factor versus $\beta^{(2)}l$ for $l = 1.0$, $\omega l/c_1 = 0.3$ and $\beta^{(1)}l = 0.4$ (Material-I/Material-I).

(v) The solution of the present paper can revert to the one of the problem which the material properties of the upper half plane and the lower half plane alone the crack line are continuous as shown in Figs 5–6 and Figs 10–12.

Acknowledgements

The authors are grateful for the financial support by the Natural Science Foundation with Excellent Young Investigators of Hei Long Jiang Province (JC04-08) and the National Natural Science Foundation of China (10572043, 10572155, 50232030, 10172030).

Appendix

The functions of $g_1(s)$, $g_2(s)$ and $g_3(s)$ can be obtained by the operation of the follow matrixes.

$$[X_1] = \begin{bmatrix} 1 & 0 & 0 \\ a_0^{(1)} & 1 & 0 \\ a_1^{(1)} & 0 & 1 \end{bmatrix}, \quad [X_2] = \begin{bmatrix} -1 & 0 & 0 \\ -a_0^{(2)} & -1 & 0 \\ -a_1^{(2)} & 0 & -1 \end{bmatrix}, \quad [X_3] = \begin{bmatrix} \mu_0^{(1)}\gamma_1^{(1)} & \gamma_2^{(1)}e_{150}^{(1)} & \gamma_2^{(1)}q_{150}^{(1)} \\ 0 & \gamma_2^{(1)}\varepsilon_{110}^{(1)} & \gamma_2^{(1)}d_{110}^{(1)} \\ 0 & \gamma_2^{(1)}d_{110}^{(1)} & \gamma_2^{(1)}\mu_{110}^{(1)} \end{bmatrix},$$

$$[X_4] = \begin{bmatrix} \mu_0^{(2)}\gamma_1^{(2)} & \gamma_2^{(2)}e_{150}^{(2)} & \gamma_2^{(2)}q_{150}^{(2)} \\ 0 & \gamma_2^{(2)}\varepsilon_{110}^{(2)} & \gamma_2^{(2)}d_{110}^{(2)} \\ 0 & \gamma_2^{(2)}d_{110}^{(2)} & \gamma_2^{(2)}\mu_{110}^{(2)} \end{bmatrix}, \quad [X_5] = [X_1] - [X_2]\,[X_4]^{-1}\,[X_3]\,,$$

$$[X_6] = \begin{bmatrix} -\mu_0^{(1)}\gamma_1^{(1)} & -\gamma_2^{(1)}e_{150}^{(1)} & -\gamma_2^{(1)}q_{150}^{(1)} \\ 0 & \gamma_2^{(1)}\varepsilon_{110}^{(1)} & \gamma_2^{(1)}d_{110}^{(1)} \\ 0 & \gamma_2^{(1)}d_{110}^{(1)} & \gamma_2^{(1)}\mu_{110}^{(1)} \end{bmatrix}, \quad [X_7] = \begin{bmatrix} x_{11}(s) & x_{12}(s) & x_{13}(s) \\ x_{21}(s) & x_{22}(s) & x_{23}(s) \\ x_{31}(s) & x_{32}(s) & x_{33}(s) \end{bmatrix} = [X_6]\,[X_5]^{-1}\,.$$

$$g_1(s) = x_{11}(s), \quad g_2(s) = x_{21}(s), \quad g_3(s) = x_{31}(s).$$

The constants of β_1, β_2 and β_3 can be obtained by the operation of the follow matrixes.

$$[Y_3] = \begin{bmatrix} \mu_0^{(1)} & e_{150}^{(1)} & q_{150}^{(1)} \\ 0 & \varepsilon_{110}^{(1)} & d_{110}^{(1)} \\ 0 & d_{110}^{(1)} & \mu_{110}^{(1)} \end{bmatrix}, \quad [Y_4] = \begin{bmatrix} \mu_0^{(2)} & e_{150}^{(2)} & q_{150}^{(2)} \\ 0 & \varepsilon_{110}^{(2)} & d_{110}^{(2)} \\ 0 & d_{110}^{(2)} & \mu_{110}^{(2)} \end{bmatrix},$$

$$[Y_5] = [X_1] - [X_2]\,[Y_4]^{-1}\,[Y_3]\,, \quad [Y_6] = \begin{bmatrix} -\mu_0^{(1)} & -e_{150}^{(1)} & -q_{150}^{(1)} \\ 0 & \varepsilon_{110}^{(1)} & d_{110}^{(1)} \\ 0 & d_{110}^{(1)} & \mu_{110}^{(1)} \end{bmatrix},$$

$$[Y_7] = \begin{bmatrix} y_{11} & y_{12} & y_{13} \\ y_{21} & y_{22} & y_{23} \\ y_{31} & y_{32} & y_{33} \end{bmatrix} = [Y_6]\,[Y_5]^{-1}\,, \quad \beta_1 = y_{11}, \quad \beta_2 = y_{21}, \quad \beta_3 = y_{31}.$$

References

[1] T.L. Wu and J.H. Huang, Closed-form solutions for the magnetoelectric coupling coefficients in fibrous composites with piezoelectric and piezomagnetic phases, *International Journal of Solids and Structures* **37** (2000), 2981–3009.

[2] J. Van Suchtelen, Product properties: a new application of composite materials, *Phillips Research Reports* **27** (1972), 28–37.

[3] G. Harshe, J.P. Dougherty and R.E. Newnham, Theoretical modeling of 3-0/0-3 magnetoelectric composites, *International Journal of Applied Electromagnetics in Materials* **4** (1993), 161–171.

[4] M. Avellaneda and G. Harshe, Magnetoelectric effect in piezoelectric/magnetostrictive multiplayer (2-2) composites, *Journal of Intelligent Material Systems and Structures* **5** (1994), 501–513.

[5] C.W. Nan, Magnetoelectric effect in composites of piezoelectric and piezomagnetic phases, *Physical Review* **B50** (1994), 6082–6088.

[6] Y. Benveniste, Magnetoelectric effect in fibrous composites with piezoelectric and magnetostrictive phases, *Physical Review* **B51** (1995), 16424–16427.

[7] J.H. Huang and W.S. Kuo, The analysis of piezoelectric/piezomagnetic composite materials containing ellipsoidal inclusions, *Journal of Applied Physics* **81**(3) (1997), 1378–1386.

[8] J.Y. Li, Magnetoelectroelastic multi-inclusion and inhomogeneity problems and their applications in composite materials, *International Journal of Engineering Science* **38** (2000), 1993–2011.

[9] G.C. Sih and Z.F. Song, Magnetic and electric poling effects associated with crack growth in $BaTiO_3$-$CoFe_2O_4$ composite, *Theoretical and Applied Fracture Mechanics* **39** (2003), 209–227.

[10] Z.F. Song and G.C. Sih, Crack initiation behavior in magnetoelectrioelastic composite under in-plane deformation, *Theoretical and Applied Fracture Mechanics* **39** (2003), 189–207.

[11] B.L. Wang and Y.W. Mai, Crack tip field in piezoelectric/piezomagnetic media, *European Journal of Mechanics. A/Solid* **22**(4) (2003), 591–602.

[12] B.L. Wang and Y.W. Mai, Fracture of piezoelectromagnetic materials, *Mechanics Research Communications* **31**(1) (2004), 65–73.

[13] C.F. Gao, P. Tong and T.Y. Zhang, Interfacial crack problems in magneto-electroelastic solids, *International Journal of Engineering Science* **41**(18) (2003), 2105–2121.

[14] C.F. Gao, H. Kessler and H. Balke, Fracture analysis of electromagnetic thermoelastic solids, *European Journal of Mechanics. A/Solid* **22**(3) (2003), 433–442.

[15] C.F. Gao, H. Kessler and H. Balke, Crack problems in magnetoelectroelastic solids. Part I: exact solution of a crack, *International Journal of Engineering Science* **41**(9) (2003), 969–981.

[16] C.F. Gao, H. Kessler and H. Balke, Crack problems in magnetoelectroelastic solids. Part II: general solution of collinear cracks, *International Journal of Engineering Science* **41**(9) (2003), 983–994.

[17] C.P. Spyropoulos, G.C. Sih and Z.F. Song, Magnetoelectroelastic composite with poling parallel to plane of line crack under out-of-plane deformation, *Theoretical and Applied Fracture Mechanics* **39**(3) (2003), 281–289.

[18] J.X. Liu, X.L. Liu and Y.B. Zhao, Green's functions for anisotropic magnetoelectroelastic solids with an elliptical cavity or a crack, *International Journal of Engineering Science* **39**(12) (2001), 1405–1418.

[19] Z.G. Zhou, L.Z. Wu and B. Wang, The dynamic behavior of two collinear interface cracks in magneto-electro-elastic composites, *European Journal of Mechanics. A/Solids* **24**(2) (2005), 253–262.
[20] Z.G. Zhou, B. Wang and Y.G. Sun, Two collinear interface cracks in magneto-electro-elastic composites, *International Journal of Engineering Science* **42** (2004), 1157–1167.
[21] K. Takagi, J.F. Li, S. Yokoyama and R. Watanabe, Fabrication and evaluation of PZT/Pt piezoelectric composites and functionally graded actuators, *Journal of the European Ceramic Society* **10** (2003), 1577–1583.
[22] D.R. Jin, Functionally graded PZT/ZnO piezoelectric composites, *Journal of Materials Science Letters* **22** (2003), 971–974.
[23] J. Chen, Z.X. Liu and Z.Z. Zou, Electriomechanical impact of a crack in a unctionally graded piezoelectric medium, *Theoretical and Applied Fracture Mechanics* **39** (2003), 47–60.
[24] B. Jin and Z. Zhong, A moving mode-III crack in functionally graded piezoelectric material: permeable problem, *Mechanics Research Communications* **29** (2002), 217–224.
[25] B.L. Wang, A mode-III crack in functionally graded piezoelectric materials, *Mechanics Research Communications* **30** (2003), 151–159.
[26] K.M. Soon, Electrical nonlinear anti-plane shear crack in a functionally graded piezoelectric strip, *International Journal of Solids and Structures* **40** (2003), 5649–5667.
[27] C.Y. Li and G.J. Weng, Antiplane crack problem in functionally graded piezoelectric materials, *Journal of Applied Mechanics* **69**(4) (2002), 481–488.
[28] J.L. Sun, Z.G. Zhou and B. Wang, Dynamic behavior of a crack in a functionally graded piezoelectric strip bonded to two dissimilar half piezoelectric material planes, *ACTA Mechanica* **176**(1–2) (2005), 45–60.
[29] Z.G. Zhou and B. Wang, Two parallel symmetry permeable cracks in functionally graded piezoelectric/piezomagnetic materials under anti-plane shear loading, *International Journal of Solids and Structures* **41** (2004), 4407–4422.
[30] Z.G. Zhou, L.Z. Wu and B. Wang, The behavior of a crack in functionally graded piezoelectric/piezomagnetic materials under anti-plane shear loading, *Archive of Applied Mechanics* **74**(8) (2005), 526–535.
[31] P.M. Morse and H. Feshbach, *Methods of Theoretical Physics,* Vol. 1, McGraw-Hill, New York, 1958.
[32] A.K. Soh, D.N. Fang and K.L. Lee, Analysis of a bi-piezoelectric ceramic layer with an interfacial crack subjected to anti-plane shear and in-plane electric loading, *European Journal of Mechanics. A/Solid* **19** (2000), 961–977.
[33] K.N. Srivastava, K.N. Palaiya and D.S. Karaulia, Interaction of shear waves with two coplanar Griffith cracks situated in an infinitely long elastic strip, *International Journal of Fracture* **23** (1983), 3–14.
[34] F. Delale and F. Erdogan, On the mechanical modeling of the interfacial region in bonded half-planes, *ASME Journal of Applied Mechanics* **55** (1988), 317–324.
[35] H. Fildis and O.S. Yahsi, The axisymmetric crack problem in a non-homogeneous interfacial region between homogeneous half-spaces, *International Journal of Fracture* **78** (1996), 139–163.
[36] M. Ozturk and F. Erdogan, Mode I crack problem in an inhomogeneous orthotropic medium, *International Journal of Engineering Science* **35** (1997), 869–883.
[37] I.S. Gradshteyn and I.M. Ryzhik, *Table of Integral, Series and Products,* Academic Press, New York, 1980.
[38] A. Erdelyi, (ed.), *Tables of Integral Transforms,* Vol. 1, McGraw-Hill, New York, 1954.